doi:10.1016/j.jmb.2007.10.073 J. Mol. Biol. (2008) 375, 875–889

JMB

Available online at www.sciencedirect.com

ScienceDirect

ELSEVIER

A Theoretical Interpretation of the Transient Sialic Acid Toxicity of a *nanR* Mutant of *Escherichia coli*

Dominique Chu[1]*, Jo Roobol[2] and Ian C. Blomfield[2]

[1]*Computing Laboratory, University of Kent, Canterbury CT2 7NF, UK*

[2]*Biomedical Research Group, Department of Biosciences, University of Kent, Canterbury CT2 7NJ, UK*

Received 11 June 2007; received in revised form 23 October 2007; accepted 25 October 2007
Available online 7 November 2007

This article reports on experimental evidence that an *Escherichia coli nanR* mutant shows inhibited growth in *N*-acetylneuraminic acid. This effect is prevented when inocula are grown in an excess of glucose, but not in an excess of glycerol. The *nanATEK* operon is controlled by catabolite repression, suggesting that diminished expression of the *nanATEK* operon in the presence of glucose explains the inocula effects. Neither double *nanR–nagC* nor *nanR dam* mutants show growth inhibition in the presence of *N*-acetylneuraminic acid. A theoretical model of *N*-acetylneuraminic acid metabolism (i.e., in particular of the *nanATEK* and *nagBACD* operons) is presented; the model suggests an interpretation of this effect as being due to transient high accumulations of GlcNAc-6P in the cell. This accumulation would lead to suppression of central metabolic functions of the cell, thus causing inhibited growth. Based on the theoretical model and experimental data, it is hypothesised that the *nanATEK* operon is induced in a two-step mechanism. The first step is likely to be repressor displacement by *N*-acetylneuraminic acid. The second stage is hypothesised to involve Dam methylation to achieve full induction.

Edited by J. Kam

Keywords: Escherichia coli; *N*-Acetylneuraminic acid; GlcNAc-6P toxicity

Introduction

Sialic acids comprise a family of nine-carbon keto amino sugars of which *N*-acetylneuraminic acid is the best studied. Largely restricted to animals and their pathogens, sialic acids commonly occupy the terminal position in glycoconjugates on eukaryotic cell surfaces. They are an important nutrient for many bacteria that colonize animal hosts, even though some, such as *Escherichia coli*, lack a sialidase and hence cannot liberate free *N*-acetylneuraminic acid from host glycoconjugates directly. In addition, microbial pathogens frequently decorate their surfaces with sialic acid as a means of circumventing host defenses; in *E. coli*, *N*-acetylneuraminic acid controls the expression of type 1 fimbrial adhesin and hence is a regulatory signal (for a recent review, see Severi *et al.*[1]).

Uptake of *N*-acetylneuraminic acid into the periplasm of *E. coli* occurs either *via* the general porins OmpF and OmpC, or *via* a selective channel (NanC).[2] NanT is required for the transport of *N*-acetylneuraminic acid across the cytoplasmic membrane, and metabolism of *N*-acetylneuraminic acid to GlcNAc-6P requires *nanATEK*.[3–6] Expression of the *nanATEK* operon is subject to catabolite repression, and hence is inhibited by glucose and is activated by Crp.[7] Furthermore, it is induced by *N*-acetylneuraminic acid, which inactivates the NanR repressor.[7] Two further steps, catalysis by NagAB and repression by the GlcNAc-6P-responsive regulator NagC, generate the central metabolic intermediate fructose-6P (Fru-6P) from GlcNAc-6P[8] (see Fig. 1).

The operator site for NanR at the *nanATEK* promoter forms part of a conserved 27-bp sequence that is also found upstream of the *nanC* gene.[9] The conserved element includes a Dam methylation site ($GATC^{NanR}$), and NanR binding to its operator prevents methylation of $GATC^{NanR}$ *in vivo* at both *nanC*[10] and *nanA* (unpublished data). Expression of both the *nanATEK* and the *nanC* operons is decreased in a *dam* mutant.[11] Furthermore, $GATC^{NanR}$ is found within a nucleotide sequence that is expected to be a relatively poor substrate for Dam

*Corresponding author. E-mail address: D.F.Chu@kent.ac.uk.

Abbreviations used: Fru-6P, fructose-6P; WT, wild type.

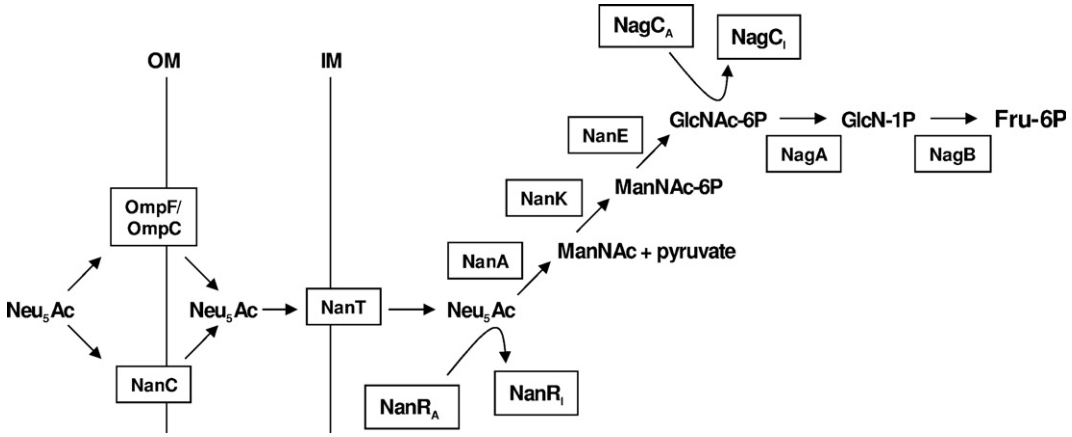

Fig. 1. Schematic representation of *N*-acetylneuraminic acid transport and metabolism; details of the pathway are described in the main text. The bacterial outer membrane (OM) and inner membrane (IM) are represented by vertical lines. Proteins are boxed, whereas *N*-acetylneuraminic acid (Neu_5Ac) and metabolic intermediates are not. Straight arrows indicate the flow of metabolic intermediates. The conversion of NanR and NagC from active repressors ($NanR_A$ and $NagC_A$) to inactivated forms ($NanR_I$ and $NagC_I$) by Neu_5Ac and GlcNAc-6P, respectively, is indicated by bent arrows. GlcN-1P enters glycolysis by conversion to Fru-6P.

methylase.[12] Thus, if methylation of $GATC^{NanR}$ controls the *nanATEK* and *nanC* promoters, full expression of these operons should be delayed until $GATC^{NanR}$ is methylated following dissociation of *NanR* from its operator sites when *N*-acetylneuraminic acid is first encountered.

In this contribution, we will provide experimental evidence that a mutation of *nanR*, depending on the inoculum, may lead to strong growth inhibition in the presence of *N*-acetylneuraminic acid. Simultaneous mutations of *nagC* or *dam* suppress this effect and lead to growth rates that are more comparable to those of the wild type (WT). We interpret the inhibited growth of the *nanR* mutant in a *N*-acetylneuraminic acid assay as a result of GlcNAc-6P accumulation in the cell; this condition has previously been shown to have toxic effects, although the mechanism of toxicity is unknown. [13]

We use a differential equation model of the control mechanisms of the *nanATEK* and *nagBACD* operons and a set of simulations in order to qualitatively explain the experimentally observed behaviour of the system. The model suggests that the toxicity is a transient effect (i.e., does not affect the long-term behaviour of the system). Furthermore, in conjunction with available experimental data, the model implies that full induction of *nanATEK* is achieved by a two-step mechanism that we propose could involve methylation of the operator site: In the first step, the turnover of *N*-acetylneuraminic acid in the cell is slowly increased during short periods of NanR displacement. The second phase is reached when methylation of the operator site allows full induction of the *nanATEK* operon. In this contribution, we suggest that this two-step induction mechanism is necessary in order for the cell to avoid high transient GlcNAc-6P accumulations (with toxic effect), while at the same time being able to benefit from high steady-state turnover rates.

Results

N-acetylneuraminic acid delays growth in a *nanR* mutant background

Expression of the *nanATEK* operon is suppressed by NanR, a FadR-like transcriptional regulator that is inactivated by *N*-acetylneuraminic acid. In the course of growth experiments, we found that rapid exponential growth in a *nanR* mutant was delayed considerably following inoculation into Mops [3-(*N*-morpholino) propanesulphonic acid] medium containing *N*-acetylneuraminic acid as the sole carbon source (Fig. 2a) and, even after 7 h, was not as rapid as the WT.

In the experiments described above, inocula were grown to saturation overnight in a glucose minimal medium containing a limiting (1.11 mM) amount of the carbon source. We reasoned that the toxic effect of *N*-acetylneuraminic acid was due to overexpression of the *nanATEK* operon in the mutant background, leading to an accumulation of excessive levels of *N*-acetylneuraminic acid, or one or more of its metabolic products. The *nanATEK* operon is suppressed by glucose (catabolite expression) independently of NanR.[7] In support of the hypothesis that overexpression of the *nanA* operon produces *N*-acetylneuraminic acid toxicity, *N*-acetylneuraminic acid toxicity was suppressed completely when the inoculum was grown overnight in a medium containing an excess of glucose (22.2 mM) (Fig. 2b). This effect was not observed when glucose was replaced by glycerol, a non-catabolite-repressing substrate (data not shown).

It has been shown previously that the accumulation of *N*-acetylneuraminic acid in a *nanA* mutant is growth inhibitory.[14] However, it seemed improbable to us that an accumulation of *N*-acetylneuraminic acid could explain *N*-acetylneuraminic acid toxicity in the *nanR* mutant, since any excess

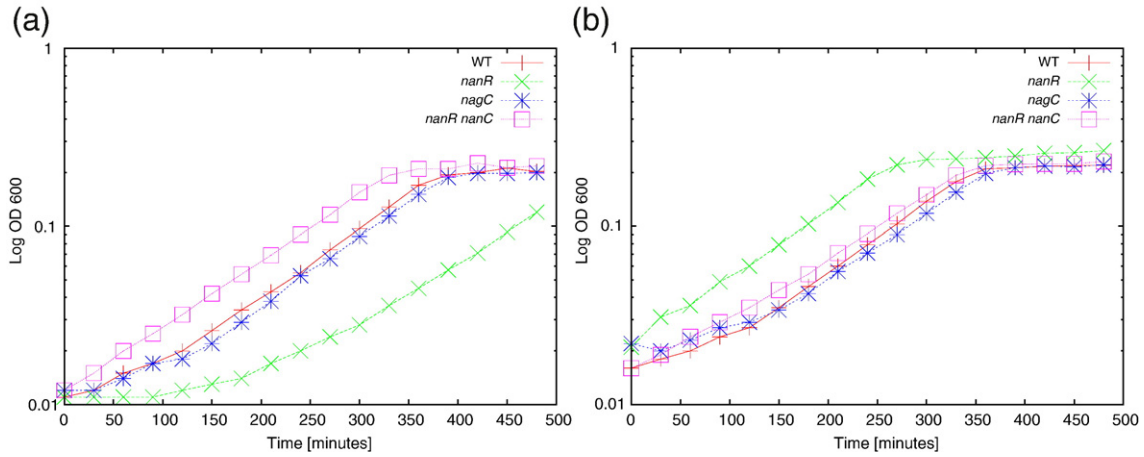

Fig. 2. Growth inhibition of a *nanR* mutant in Mops minimal medium containing *N*-acetylneuraminic acid. The WT or mutant strain indicated was inoculated following overnight growth in Mops minimal medium containing (a) 1.11 mM or (b) 22.2 mM glucose as the sole carbon source. The cultures were incubated at 37 °C with rapid aeration. The growth of the WT and the mutant strains indicated was monitored spectrophotometrically at 600 nM.

N-acetylneuraminic acid taken up by NanT in the *nanR* mutant should be converted rapidly to GlcNAc-6P by the concerted actions of the NanA, NanE, and NanK. On the other hand, GlcNAc-6P is also known to be toxic,[13] and we reasoned that low initial induction of the *nagBACD* operon, and hence an accumulation of GlcNAc-6P, would more likely be responsible for *N*-acetylneuraminic acid toxicity. In support of this hypothesis, a secondary mutation in the *nagBACD* operon repressor *nagC* suppressed completely the toxic effects of *N*-acetylneuraminic acid in the *nanR* mutant (Fig. 2b). The mechanism of GlcNAc-6P toxicity is unknown, but is thought to involve a lack of intermediary metabolites.[13] Consistent with this hypothesis, no growth defect was observed in a *nanR* mutant grown in a Mops-rich defined medium that contains exogenous bases and amino acids (data not shown).

Expression of *nanA* is activated by Dam methylation.[15] To probe further the potential role of Dam methylation in the regulation of the *nanA* operon, the ability of a *dam* mutation to suppress the effect of *N*-acetylneuraminic acid on the *nanR* mutant was also examined (Fig. 3). It was found that the *dam* mutant restored the growth rate of the *nanR* mutant to near-WT levels. This result supports the hypothesis that overexpression of the *nanA* operon produces *N*-acetylneuraminic acid toxicity. Furthermore, it indicates that if methylation of GATC$^{\text{NanR}}$ activates the expression of the *nanA* operon, then this effect occurs even in the absence of NanR.

Theory

Formulation of the Base, Extended, and Full Models will introduce three variants of a model of *N*-acetylneuraminic acid metabolism in *E. coli*. The first ("base") model makes a number of simplifying assumptions, but provides some intuition about the behaviour of the system. The second ("extended") model extends the base model by taking into account the transcription/translation step in gene expression. Finally, the third ("full") model refines the extended model by introducing more realistic

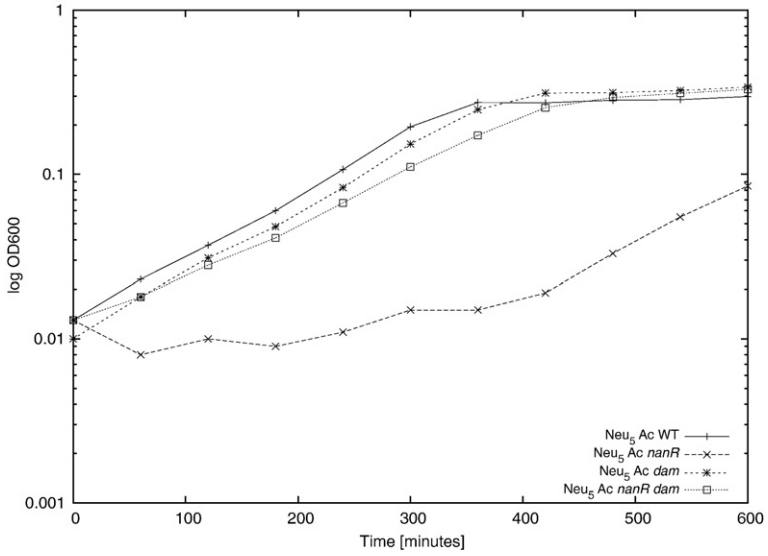

Fig. 3. Suppression of *N*-acetylneuraminic acid toxicity in a *nanR* mutant by simultaneous mutation of *dam*. The WT or the mutant strains indicated were inoculated into fresh Mops minimal medium containing *N*-acetylneuraminic acid as the sole carbon source following overnight growth in Mops minimal medium containing 1.11 mM glucose as the sole carbon source. The cultures where incubated at 37 °C with rapid aeration. The growth of the WT and the mutant strains indicated was monitored spectrophotometrically at 600 nM.

kinetics. This latter model is more complex than the base and extended models, but shows the same qualitative behaviour (at least for the purpose of the current contribution).

Formulation of the base, extended, and full models

Our base model is defined by the following set of differential equations (Tables 1 and 2):

$$\dot{s}_1 = 0 \tag{1}$$

$$\dot{x}_1 = rs_1 - rs_2 \tag{2}$$

$$\dot{e}_1 = re_1 - c_{e_1}e_1 \tag{3}$$

$$\dot{s}_2 = rs_2 - rx_2 \tag{4}$$

$$\dot{e}_2 = re_2 - c_{e_2}e_2 \tag{5}$$

where the parameters of the system are defined in Table 3. This model describes the flow of external (periplasmic) *N*-acetylneuraminic acid (s_1) into the cytoplasm (Eqs. (1) and (2)) *via* NanT (here represented by e_1). Cytoplasmic *N*-acetylneuraminic acid is denoted by x_1; its breakdown into GlcNAc-6P (represented by s_2) is catalysed by e_1. Differing concentrations of NanA/NanB and NanT are taken care of by the relevant constants describing uptake and metabolic efficiencies. Regulation of the uptake and metabolism of *N*-acetylneuraminic acid is represented in the model by the transcription efficiency g (see Table 3) describing the activity of *nanATEK*. If $g=0$, then no e_1 is produced, and hence no *N*-acetylneuraminic acid is taken up or metabolized, whereas $g=1$ describes the case of full *nanATEK* derepression and e_1 is produced at its maximum rate (defined by the value of V_{e_1}). Generally, a higher nR (representing the amount of NanR) leads to a lower g, and a higher x_1 leads to a higher g.

Equations (4) and (5) are the GlcNAc-6P counterparts of Eqs. (2) and (3). The symbol e_2 represents the products of the *nagBACD* operon. The autorepressive activity of NagC is reflected in the transcription efficiency g_2 (see Table 3). Like its counterpart g, g_2 varies between 0 and 1. The higher is e_2, the lower is g_2. Yet, the higher is g_2, the higher are the expression levels of e_2. Similarly, the more s_2 (GlcNAc-6P) there is in the system, the higher is g_2. The details of the GlcNAc-6P breakdown (and its products) are not represented in this model.

This model contains a number of simplifying assumptions. In particular, the influx of *N*-acetylneuraminic acid into the periplasm is not explicitly modelled because *N*-acetylneuraminic acid diffuses through the outer cell wall through the nonspecific OmpF/OmpC porin;[2] uptake into the periplasm is therefore only weakly regulated. Other simplifying assumptions include the following:

- The model reduces the metabolism of *N*-acetylneuraminic acid (see Fig. 1) to a two-step process.
- The metabolic enzymes encoded by *nanATEK* and *nagBACD* are summarised by e_1 and e_2, respectively. Essentially, this amounts to assuming that the concentrations of the proteins expressed from the same operon are in a fixed ratio.

These simplifications can be justified by considering that (i) they facilitate the mathematical interpretation and treatment of the model. Furthermore, (ii) this article only considers qualitative models; simplifications resulting in quantitative inaccuracies are inconsequential. Finally, (iii) more complex models would also introduce a number of additional unknown parameters; these would need to be guessed and, by themselves, introduce additional uncertainties.

The base model (i.e., Eqs. (1)–(5)) does not represent mRNA expression. An extended model that represents the mRNA expression is identical with the base model, except for the following replacement of and addition to Eqs. (1)–(5) (Tables 4–7):

$$\dot{\varrho}_{e_1} = d^{\varrho}_{e_1}(re_1 - \varrho_{e_1}) \tag{6}$$

$$\dot{e}_1 = \varrho_{e_1} - c_{e_1}e_1 \tag{7}$$

$$\dot{\varrho}_{e_2} = d^{\varrho}_{e_2}(re_2 - \varrho_{e_2}) \tag{8}$$

$$\dot{e}_2 = \varrho_{e_2} - c_{e_2}e_2 \tag{9}$$

Note that the steady-state solutions of the extended model are identical with those of the base model. From a dynamical point of view, the main difference between the models is that production of mRNA—here denoted as ϱ_{e_x} (where $x=1, 2$)—introduces a delay into the system. The size of the delay will crucially depend on the translation efficiency of the enzymes $d^{\varrho}_{e_x}$.

The extended model assumes that (i) mRNA breakdown is negligible, and (ii) proteins are degraded at a fixed rate. These assumptions are not necessarily correct (e.g., see Narang[16] and Narang

Table 1. Summary of the main symbols used

s_1	*N*-acetylneuraminic acid (external)
e_1	Products of *nanATEK*
s_2	GlcNAc-6P
nR	NanR (kept fixed)
x_1	*N*-acetylneuraminic acid in the cytoplasm
e_2	Products of *nagBACD*
ϱ_{e_x}	mRNA for enzyme e_x
g_x	Transcription efficiency of *nanATEK* and *nagBACD*

Table 2. Summary of the main symbols used

s_1	*N*-acetylneuraminic acid (external)
e_1	Products of *nanATEK*
s_2	GlcNAc-6P
nR	NanR (kept fixed)
x_1	*N*-acetylneuraminic acid in the cytoplasm
e_2	Products of *nagBACD*
ϱ_{e_x}	mRNA for enzyme e_x
g_x	Transcription efficiency of *nanATEK* and *nagBACD*

Table 3. Definition of the dynamical parameters used in the model of *N*-acetylneuraminic acid metabolism

$g \doteq \frac{k_2 + k_3 x_1}{k_2 + k_3 x_1 + k_1 nR}$	$g_2 \doteq \frac{l_2 + l_3 s_2}{l_2 + l_3 s_2 + l_1 e_2}$
$re_1 \doteq g V_{e_1}$	$re_2 \doteq g_2 V_{e_2}$
$rs_1 \doteq V_{s_1} e_1 \frac{s_1}{K_{s_1} + s_1}$	$rs_2 \doteq V_{s_2} e_1 \frac{x_1}{K_{x_1} + x_1}$
$rx_2 \doteq V_c e_2 \frac{s_2}{K_{s_2} + s_2}$	c_{e_x}—protein breakdown coefficient

The parameter k_1 describes the affinity of nR for the operator site, k_2 is the dissociation constant, and k_3 is a constant describing the efficiency of nR displacement by x_1. The parameters l_x have an analogous interpretation for e_2 and s_2. Vs_1, Vs_2, and Vs_c are the enzymatic rates for *N*-acetylneuraminic acid transport into the cytoplasm (i.e., the $s_1 \rightarrow x_1$ conversion), the rate of *N*-acetylneuraminic acid breakdown, and the rate of GlcNAc-6P breakdown, respectively. The parameters K_x are saturation parameters. The transcription efficiencies g,g_2 are derived under the assumption that displacement of the repressor is a one-step process (i.e., no intermediate repressor–derepressor–nucleotide compounds are formed; see Appendix A for the derivation). All parameters are constant and positive; in this contribution, we restricted the value of the parameters to the interval (0, 1) (see Materials and Methods for an explanation).

and Pilyugin[17]). A more realistic model would take into account the limited lifetime of mRNA and replace fixed-rate protein breakdown with a model where protein is diluted by cell growth (i.e., proportional to the efflux of GlcNAc-6P given by rx_2). The resulting model (which we will henceforth refer to as the full model) is then obtained by replacing Eqs. (6)–(9) with the following:

$$\dot{\varrho}_{e_1} = d^{\varrho}_{e_1}(re_1 - \varrho_{e_1}) - c_{\varrho}\varrho_{e_1} \tag{6'}$$

$$\dot{e}_1 = \varrho_{e_1} - rx_2 c_{e_1} e_1 \tag{7'}$$

$$\dot{\varrho}_{e_2} = d^{\varrho}_{e_2}(re_2 - \varrho_{e_2}) - c_{\varrho}\varrho_{e_2} \tag{8'}$$

$$\dot{e}_2 = \varrho_{e_2} - rx_2 c_{e_2} e_2 \tag{9'}$$

The breakdown of mRNA with constant c_{ϱ} is represented by the last terms in Eqs. (6′) and (7′).

Derivation of steady-state values

In what follows, we will calculate the steady state of the base model (which is identical with the steady state of the extended model).

From Eq. (3), we can calculate steady-state values for e_1:

$$gV_{e_1} - c_{e_1} e_1 = V_{e_1} \underbrace{\frac{k_2 + k_3 x_1}{k_2 + k_3 x_1 + k_1 nR}}_{\doteq \beta} - c_{e_1} e_1 = 0$$

$$\rightarrow \beta V_{e_1} - c_{e_1} \beta e_1 - c_{e_1} k_1 nR e_1 = 0$$

$$\rightarrow e_1 = \frac{\beta V_{e_1}}{\beta c_{e_1} + c_{e_1} k_1 nR} \tag{10}$$

Similarly, using Eq. (2), we can calculate the steady-state concentration of x_1:

$$rs1 - rs2 = 0 = V_{s_1} e_1 \left(\underbrace{\frac{s_1}{K_{s_1} + s_1}}_{\doteq \sigma} \right) - V_{s_2} e_1 \frac{x_1}{K_{x_1} + x_1} \tag{11}$$

$$\rightarrow x_1 = \frac{V_{s_1} \sigma K_{x_1}}{V_{s_2} - V_{s_1} \sigma} \tag{12}$$

Due to the assumption that the metabolic proteins NanA and NanB and the transporter NanT are in a fixed ratio, in this model, the concentration of *N*-acetylneuraminic acid (x_1) in the cytoplasm is independent of the induction level of the *nanATEK* operon (i.e., e_1); this is clear from Eq. (12). The amount of e_1 regulates the turnover rate of *N*-acetylneuraminic acid (i.e., how fast it is taken up and converted into GlcNAc-6P). Hence, the level of x_1 is only determined by the parameters of the system and by the amount of *N*-acetylneuraminic acid in the periplasm.

Using Eq. (4), we obtain a steady-state value for s_2—the GlcNAc-6P concentration in the cytoplasm. Setting $\alpha \doteq \left(\frac{x_1}{K_{x_1} + x_1} \right)$, we get:

$$rs_2 - rx_2 = 0 = Vs_2 e_1 \alpha - V_c e_2 \frac{s_2}{K_c + s_2}$$
$$\rightarrow V_{s_2} e_1 \alpha K_c + V_{s_2} e_1 \alpha s_2 - V_c e_2 s_2 = 0$$

$$\rightarrow s_2 = \frac{V_{s_2} e_1 \alpha K_c}{V_c e_2 - V_{s_2} e_1 \alpha} \tag{13}$$

Here, s_2 is a function of the inducers e_1, e_2, and x_1. Keeping everything else fixed, an increase in e_1 (*nanATEK* induction) will lead to an increase in s_2 (GlcNAc-6P concentration); increasing e_1, however, can only continue as long as the denominator in Eq. (13) remains greater than zero. An increase beyond this point will lead to an undefined steady state (i.e., an unstable model). Apart from e_1, the steady-state concentration of GlcNAc-6P also depends on the external/periplasmic, but not the cytoplasmic, *N*-acetylneuraminic acid concentration.

Necessary conditions for the stability of WT

For reasons of biological plausibility, we assume that the WT will normally operate in a stable dynamical regime (see Computational Simulations for a discussion of what we mean by stability). The above steady-state analysis allows one to establish some necessary conditions for the existence of stable solutions:

- From Eq. (12): $V_{s_2} > \sigma V_{s_1}$. This essentially means that the speed with which *N*-acetylneuraminic acid is converted must be higher than the speed with which it is brought into the system.

- From Eq. (13): $V_c e_2 > V_{s_2} e_1 \alpha$. This means that the influx of GlcNAc-6P must be lower than its efflux (i.e., metabolic breakdown).

Independent of the parameters, the model has, at most, one steady-state solution (see Appendix A).

Results for the nanR single mutant

The *nanR* mutant corresponds to the limiting case of $nR \ll k_2 + k_3 x_1$. In this case, e_1 will approach the steady-state value:

$$e_1^{nR} = V_{e_1}/c_{e_1} \tag{14}$$

Clearly, $e_1^{nR} > e_1$ for any positive nR, confirming the intuitive expectation that the turnover of *N*-acetylneuraminic acid is strictly higher in the *nanR* mutant than in the WT. As a consequence of the higher levels of e_1 in the mutant, it can be seen from Eq. (13) that the steady-state values of s_2 will be higher than in the WT. Note, however, that this model predicts that the *N*-acetylneuraminic acid concentration in the cytoplasm will not be affected by the mutation.

Double mutant

The *nanR–nagC* double mutant can be calculated exactly. It is defined by $g_2 = 1$ and $nR = 0$. In this case, all variables take very simple solutions in terms of their parameters. The concentrations of e_1 and e_2 can be obtained from Eqs. (3) and (5), respectively:

$$e_1 = \frac{V_{e_1}}{c_{e_1}}, \quad e_2 = \frac{V_{e_2}}{c_{e_2}} \tag{15}$$

The steady-state amount of s_2 can be obtained from Eq. (4):

$$s_2 = \frac{V_{s_2} \frac{V_{e_1}}{c_{e_1}} \alpha K_c}{V_c \frac{V_{e_2}}{c_{e_2}} - V_{s_2} \frac{V_{e_1}}{c_{e_1}} \alpha} \tag{16}$$

Note that, in the limit of very large s_2, the single mutant will show the exact same behaviour as the double mutant because $g_2 \to 1$ for large s_2.

Simulations

Approach of steady state in the extended model

As long as one is only interested in the steady-state values, the basic model of Eqs. (1)–(5) and the extended model of Eqs. (1)–(9) are identical. These models differ, however, in how they approach the steady state. The transcription step introduces an additional delay into the system that potentially modifies the transient behaviour of the model.

In what follows, we will (unless stated otherwise) assume initial conditions corresponding to very low (or vanishing) enzyme (i.e., e_1 and e_2) and mRNA concentrations. In the case of the basic model, there are only small delays in the system (depending on the specific parameters), and the cytoplasmic steady-state concentrations of x_1 and s_2 (*N*-acetylneuraminic acid and GlcNAc-6P, respectively) are approached from below (i.e., the steady-state concentration is the maximum, or is close to the maximum, concentration reached). If the delay in the system is significant, then the transient concentrations of s_2 and/or x_1 will initially overshoot their steady-state concentrations by possibly quite large amounts. In the extended model, the parameter that determines the delay resulting from mRNA expression is $d_{e_x}^{\varrho}$.

Figures 4 and 5 show how the steady state is approached depending on the size of the delay in the extended model. For a value of $d_{e_x}^{\varrho} = 0.1$, the system in Fig. 4 shows no significant overshoot of the steady-state values. Both the WT and the single *nanR* mutant approach their respective steady states from below. With increased delay (i.e., decreasing the value of $d_{e_x}^{\varrho}$), the qualitative behaviour changes, and both the WT and the mutant show transient accumulations of s_2 before the steady-state value is reached. For long delays, these accumulations can be very significant compared to the steady state. Accumulations occur in both the WT and the mutant, but in the particular case of Fig. 4, the accumulation in the mutant is higher than in the WT by a factor of 4. Note that, in the extended model, the steady-state value is independent of the delay $d_{e_x}^{\varrho}$.

Similarly, for the parameters used in Fig. 5, the *nanR* mutant shows a transient accumulation of s_2 by a factor of >60 compared to the steady-state value for a delay of $d_{e_x}^{\varrho} = 0.001$. Yet again, no accumulation occurs in the simulation of the *nanR–nagC* double mutant.

Stability of qualitative behaviour: The full model

While the full model is somewhat more complicated to analyse when compared to the base or extended model, most of the intuition developed for the base model can be carried over to the full model as well. What is more important, however, is that the full model approaches steady state qualitatively in the same way as the extended model does. The model shows an overshoot of s_2 that depends on the delay in gene expression. Figure 6 is an example; here, the overshoot of s_2 is relatively modest, and the difference between WT and mutant is small. For different parameters, such as in Fig. 7, the model demonstrates a very large difference in transient GlcNAc-6P concentrations in the WT and the mutant.

Discussion

N-Acetylneuraminic acid is a carbon source for *E. coli* that can be metabolized into GlcNAc-6P and Fru-6P, eventually fueling the growth of the organism. However, our results show that too rapid utilization

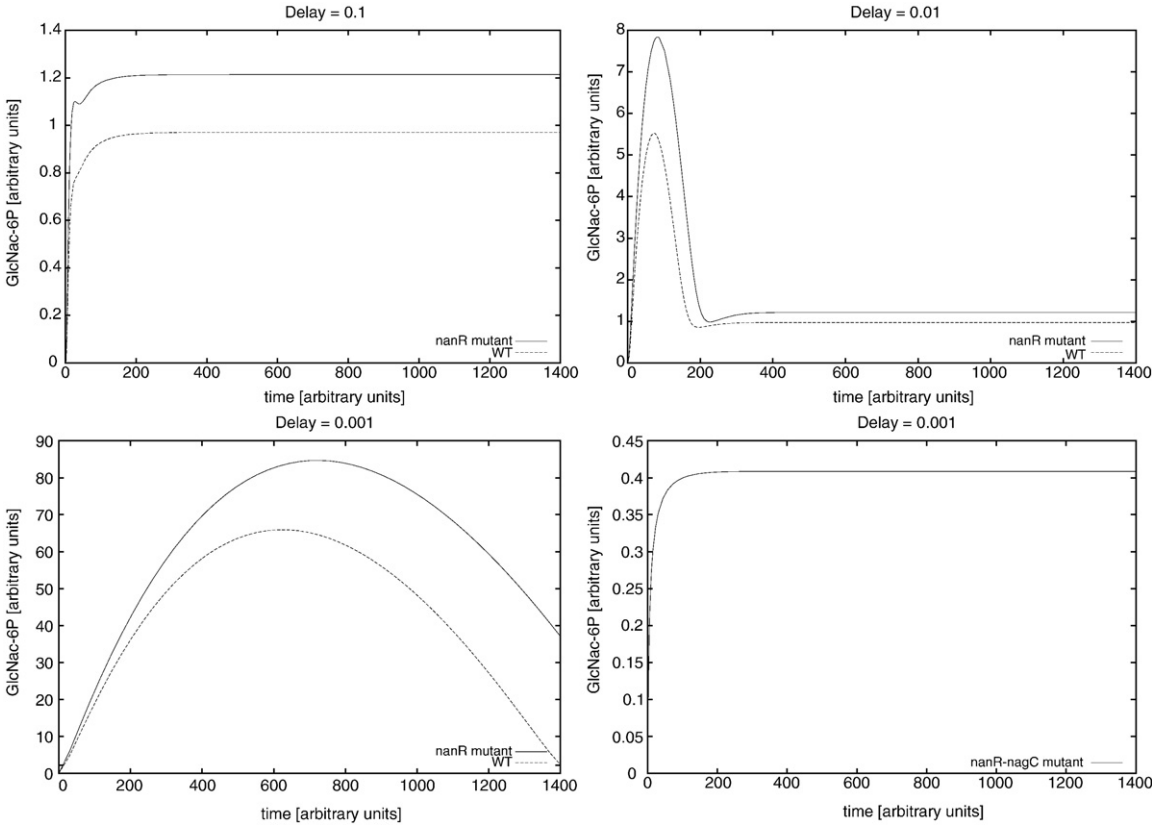

Fig. 4. Comparison of how GlcNAc-6P approaches steady state for different delays and a different set of parameters. The double mutant (bottom right) approaches the steady state from below even for significant delays. For the parameters of this simulation, see Table 4.

of *N*-acetylneuraminic acid can lead to growth inhibition, depending upon the growth conditions prior to *N*-acetylneuraminic acid exposure. We will henceforth assume that this toxic effect is caused by GlcNAc-6P.

In this section, we will interpret (and connect) the experimental, theoretical, and simulation results reported in Results; we will also discuss how they can be understood in the light of previous results. The main conclusion is a prediction that *nanATEK* will be regulated in a two-step process, in that full induction of the gene is only reached after an initial period with intermittent induction. The rationale is that, by using this two-step process, the cell can efficiently metabolize *N*-acetylneuraminic acid and GlcNAc-6P in steady state while avoiding the toxic effects of transient (high) accumulations of GlcNAc-6P.

Steady-state behaviour does not explain GlcNAc-6P toxicity

The lack of growth of the *nanR* mutant cannot be explained by the steady-state properties of this (or indeed any other possible) model. To see this, consider the two possible scenarios that could explain the observed experimental evidence:

(1) The mutant has a steady-state GlcNAc-6P concentration that is high enough to cause toxicity, whereas the concentration in the WT is too low to show any symptoms.
(2) The WT has a nontoxic steady state, but in the mutant, GlcNAc-6P grows without bounds (i.e., it does not have a steady state). Translated into the language of dynamical systems, this would mean that the WT shows stable behaviour, but the mutant is unstable.

A priori, both scenarios are plausible *vis-à-vis* the mathematical model: There are sets of parameters where the WT has a steady state but the mutant does not; even if the mutant has a steady-state GlcNAc-6P concentration, for many sets of parameters, it will be much higher than the WT concentration, thus potentially causing the toxic effect.

We think that a steady-state explanation is not correct for the following reasons: Firstly, the parameters leading to a stable WT and an unstable mutant are rare in the parameter space of the extended model (we estimated them to be about 3%; see Appendix A). However, this estimate is most certainly dependent on one of our modelling assumptions, namely, that $nR = 0.7$ (which we left fixed). Increasing this value would lead to an increase in the proportion of models with stable WT but unstable mutant. Moreover, one cannot *a priori* exclude that evolution chose a rare set of parameters.

A stronger argument is provided by the second reason: While a small proportion of parameter space

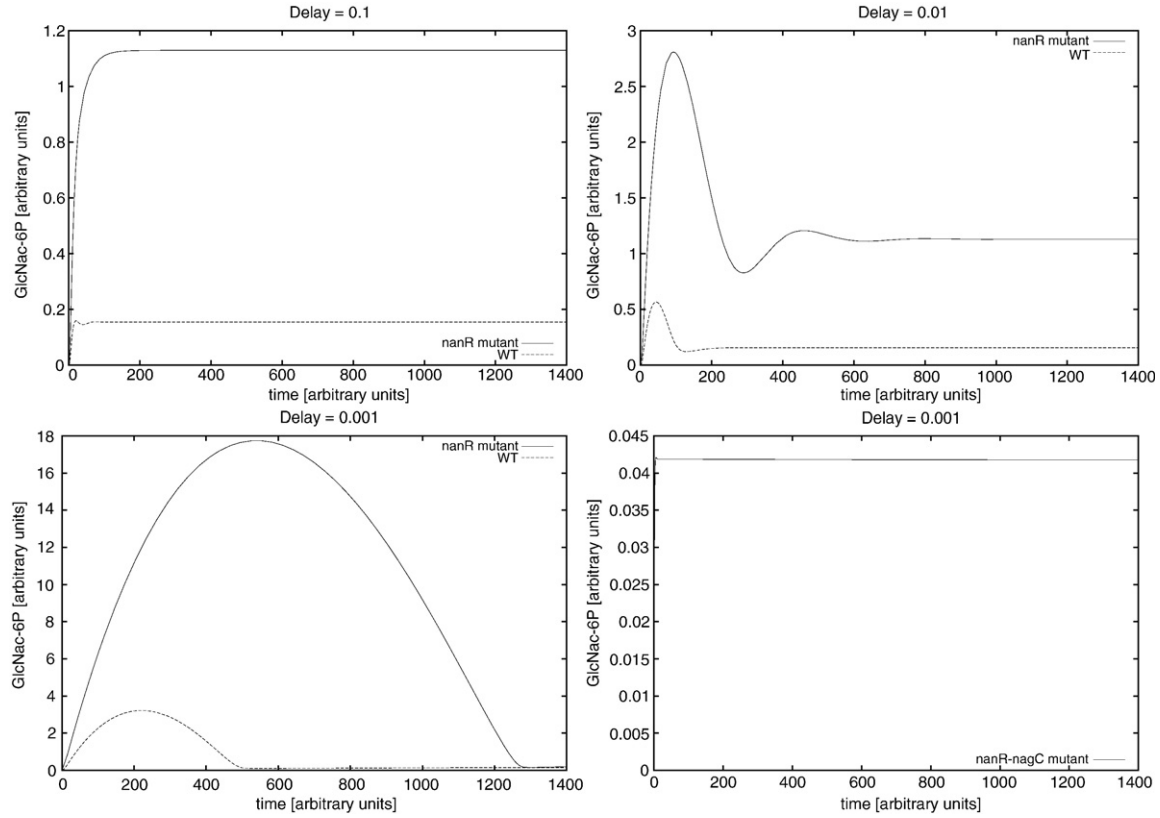

Fig. 5. Comparison of how s_2 approaches steady state for different values of the (delay) parameter $d^{o}_{\hat{e}_2}$. This is an example simulation. The quantitative details depend on the parameters chosen for the model (listed in Table 5); however, the qualitative trend of increased transient accumulations for longer delays is independent of the parameters.

supports stable behaviour for the WT and unstable behaviour for the *nanR* mutant, we did not find a single set of parameters where the WT and single mutant are stable and unstable, respectively, but the double *nanR–nagC* mutant is stable. This suggests that the stable–unstable–stable combination is at least extremely rare or even nonexistent. Theoretically, one would indeed not expect to find a stable–unstable–stable configuration because the model predicts the *nanR* mutant and the double *nanR–nagC* mutant to be equivalent for large s_2 (because $g_2 \to 1$ for $s_2 \to \infty$; i.e., the *nagBACD* operon is completely derepressed at high concentrations of GlcNAc-6P).

Thirdly, experimental evidence directly suggests non-steady-state explanations. The toxic effect experienced by the *nanR* mutant is transient in the sense that the population recovers and returns to near-normal growth after a certain period (see Fig. 2) (i.e., there is no observable toxic effect of GlcNAc-6P in the long run). Steady-state explanations would only describe the behaviour of the system in the long term.

Fourthly, in systems where there is only one stable steady state, the long-term behaviour of the system is independent of the initial conditions of the system. Yet in the experiments, the toxic effect is only seen in carbon-starved inocula, but not in inocula grown in carbon-rich conditions. In the mathematical model, different inoculations manifest themselves in different initial conditions. If a system has a steady state that is unique and stable, then its long-term behaviour does not depend on its initial conditions. Hence, the fact that the appearance of toxicity depends on the inoculum indicates that the effect is not due to the steady-state behaviour of the system.

In summary, mathematical and experimental evidence indicates strongly that GlcNAc-6P toxicity in the *nanR* mutant is a transient effect. Steady-state GlcNAc-6P levels are nontoxic in the WT, in the *nanR* mutant, and in the double *nanR–nagC* mutant.

An *ansatz* based on transient behaviour

Rather than being due to the steady-state properties of the system, we suggest a model based on transient accumulations of GlcNAc-6P and subsequent toxicity effects. The explanatory *ansatz* can be summarised as follows:

- Upon exposure to external *N*-acetylneuraminic acid, transient GlcNAc-6P concentrations transiently rise to high levels both in the WT and in the *nanR*. These transient accumulations tend to increase when a delay in the *nagBACD* gene expression is introduced.
- The mathematical models can explain the experimentally observed transient toxicity of the *nanR* mutant (and its absence in the WT) when

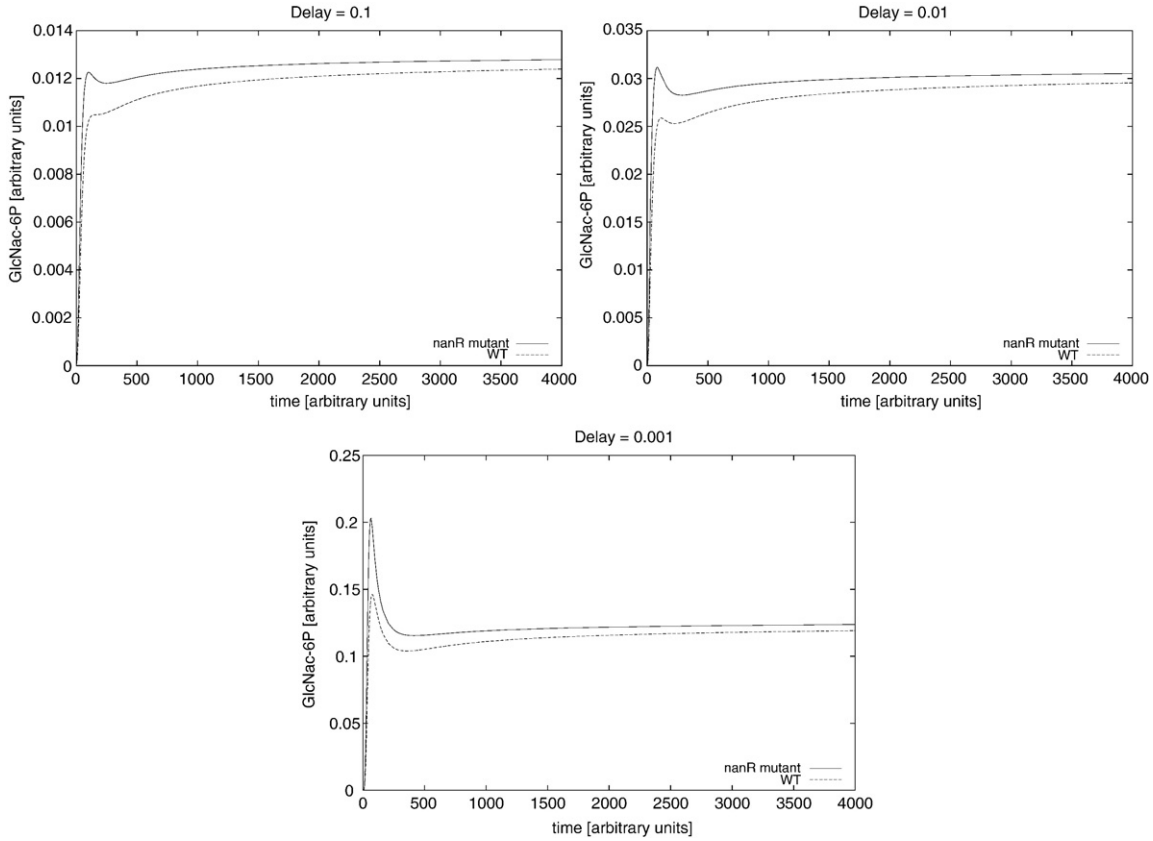

Fig. 6. Comparison of how s_2 approaches steady state for different values of the (delay) parameter $d^o_{e_x}$ for the full model. Here, *nanR* repression is efficient; hence, there is a smaller transient effect (see parameters in Table 6).

transient NanATEK levels are low in the WT but high in the mutant.

- A large difference in transient NanATEK concentrations between the *nanR* mutant and the WT can be explained when *nanATEK* derepression by *N*-acetylneuraminic acid is inefficient.
- This suggests a two-step model of *nan* induction, whereby full induction levels of the operon are only reached after a period of gradual buildup of enzyme levels in the cell. This two-step mechanism can avoid toxicity in the WT while still allowing full utilization of the carbon source.
- This explains available experimental evidence (i.e., the experiments with the *dam* mutant in Fig. 3 and data from the literature, especially Kalivoda *et al.*[7]).

In the remainder of this section, we will justify this model in detail.

Delays cause transient accumulations, but not in the double mutant

The two most relevant qualitative features of both the extended and the full models are as follows: (i) The transient GlcNAc-6P accumulations in the extended/full model last longer and are greater the longer the delays (see Figs. 4–7). (ii) Independent of the delay, the *nanR–nagC* mutant approaches the steady-state GlcNAc-6P concentration from below (i.e., shows no transient accumulations of s_2; GlcNAc-6P).

An interpretation of experimental data based on the assumption that GlcNAc-6P toxicity is a transient phenomenon immediately explains aspects of the available data: The toxicity effect in the *nanR* mutant, one can hypothesize, is caused by transient accumulations of GlcNAc-6P, which in turn are caused by a (normal) delay in induction of the system. Once the toxic limit is reached, this normal delay is exacerbated by even higher GlcNAc-6P accumulations until eventually the cell manages to return to normal function. In the double mutant, the *nagBACD* operon will always be fully expressed (due to the absence of the repressing NagC), hence steady-state concentrations of the relevant enzymes will be reached; breakdown of the GlcNAc-6P commences without delay upon the cell's exposure to *N*-acetylneuraminic acid.

This *ansatz* has a potential problem apparent from Figs. 4 and 6: Unlike the solutions in Figs. 5 and 7, GlcNAc-6P accumulates in these simulations to similar levels in both the WT and the *nanR* mutant. This suggests that there are regions in parameter space where both the WT and the *nanR* mutant transiently accumulate toxic concentrations of GlcNAc-6P. This leaves a crucial aspect of the model underexplained, namely, the experimentally observed difference in qualitative behaviour between the WT and the single mutant.

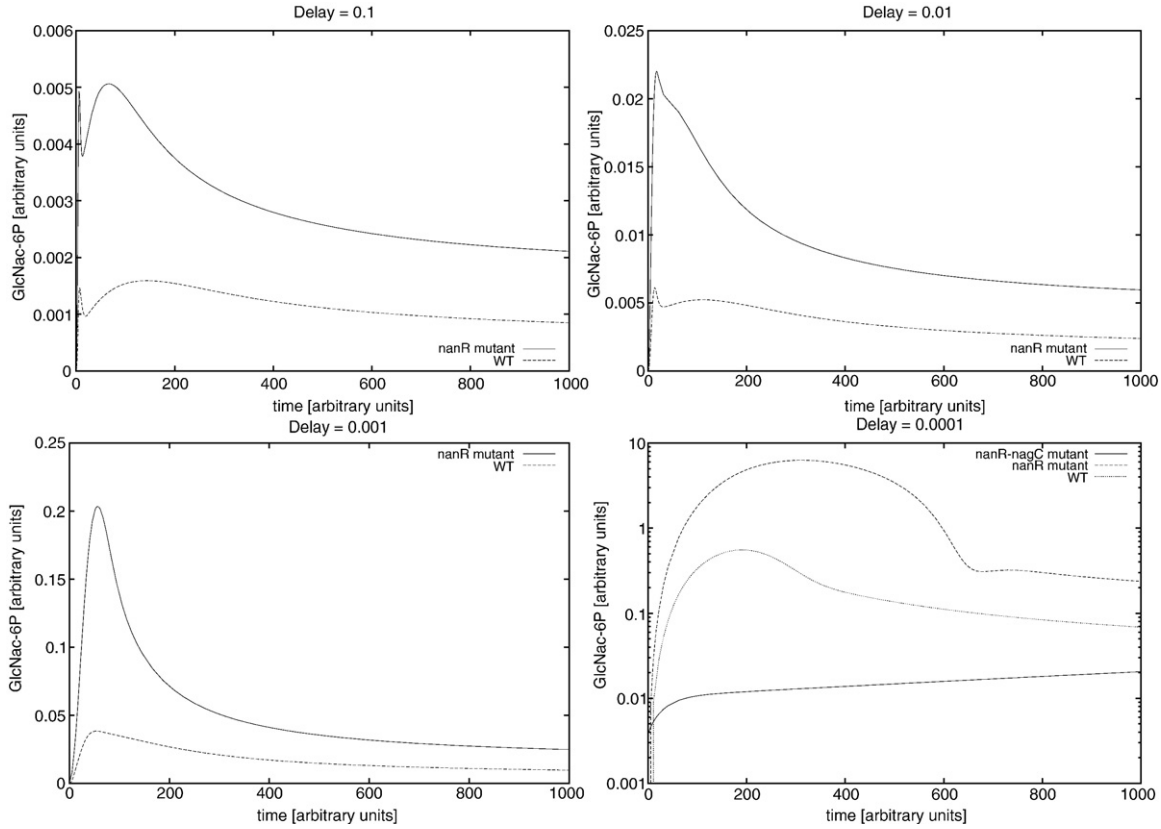

Fig. 7. Comparison of how s_2 approaches steady state for different values of the (delay) parameter $d_{e_x}^{Q}$ for the full model. Here, *nanR* repression is inefficient (see parameters in Table 7); hence, there is a large transient effect. The last panel shows s_2 on a log scale because of the great differences between the three curves.

One possible explanatory strategy is to simply acknowledge that the parameters of the real systems happen to be such that the WT does not display a high transient GlcNAc-6P accumulation while the *nanR* mutant does (clearly, there are parameters that support this). The force of this argument is, in fact, much stronger than it seems at a first glance: The absence of toxic GlcNAc-6P accumulations in the WT *per se* does not require any explanation because toxicity impairs viability. What remains to be explored, at this point, is under which conditions the system would accumulate high transient GlcNAc-6P concentrations in the mutant, while the WT only shows small accumulations.

In Figs. 4 and 5 (for the extended model) and in Figs. 6 and 7 (full model), the GlcNAc-6P accumulation in the mutant is always higher than in the WT. Theoretically, this is expected to be the case for all possible parameter sets because the *nanR* mutant has a higher influx of GlcNAc-6P than the WT, while the regulation of the GlcNAc-6P metabolism is assumed to be the same as in the WT. Yet, the difference between the accumulation in the WT and the accumulation in the mutant will crucially depend on the parameters of the system; it could range from very small to very large (as illustrated by the examples in Figs. 4–7). This leads to two questions: (i) Theoretically, which parameters determine the difference in transient behaviour? (ii) Are there any plausible biological reasons to expect a big/small difference in transient GlcNAc-6P between the WT and the mutant in the cell?

Addressing (ii) first, biologically, it is plausible to expect that the maximum GlcNAc-6P concentration in the WT will be well below toxic levels. If steady-state GlcNAc-6P values in the WT were close to the toxic limit, random fluctuations would take the cell over this limit. Combined with the experimental evidence on growth inhibition in the mutant, this suggests that the difference between maximum transient GlcNAc-6P accumulation in the WT and maximum transient GlcNAc-6P accumulation in the *nanR* mutant should be large.

What determines transient GlcNAc-6P accumulations?

In order to get a better theoretical understanding of the conditions that lead to a large difference in transient GlcNAc-6P levels, consider that the maximum transient GlcNAc-6P accumulation will depend on the rate of GlcNAc-6P synthesis (i.e., GlcNAc-6P influx) and its breakdown rate (i.e., efflux). Assuming (for the moment) a fixed efflux mechanism, then accumulation levels will mainly depend on the *N*-acetylneuraminic acid turnover rate. This rate itself depends on the induction levels

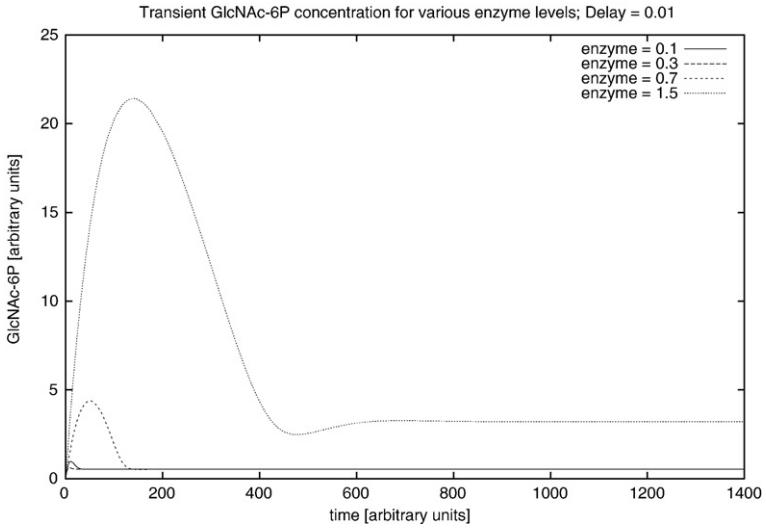

Fig. 8. The transient values of GlcNAc-6P depend on the concentration of the enzyme regulating *N*-acetylneuraminic acid throughput. In these simulations, x_1 was kept constant at 1, and e_1 was set to various levels ranging from 0.3 to 1.5. Enzyme levels will be high in the *nanR* mutant compared to the WT if NanR is an effective repressor over physiological levels of *N*-acetylneuraminic acid (see the main text for details).

of *nanATEK* (e_1 in the model). Figure 8 shows s_2 (i.e., GlcNAc-6P) accumulations for various levels of e_1; in this graph, the parameters regulating the breakdown of s_2 have been kept constant. The figure clearly illustrates that (at least for this particular set of parameters) increasing the amount of e_1 leads to a higher transient GlcNAc-6P accumulation. Fig. 8 only describes the behaviour of a specific set of parameters for GlcNAc-6P breakdown. However, any set of parameters will show a qualitatively similar trend, with only the quantitative details (i.e., the absolute values of s_2 accumulation) being different. In terms of the regulation of the GlcNAc-6P metabolism, a high difference in e_1 in the model translates into a high difference in *nanATEK* repression in the cell between the WT and the *nanR* mutant. Since the *nanR* mutant is fully derepressed, this means that the WT is, at most, partially induced even in the presence of external *N*-acetylneuraminic acid. In short, the difference in transient GlcNAc-6P levels between the WT and the mutant will be big if *N*-acetylneuraminic acid does not efficiently derepress *nanATEK*.

In the full model, the same qualitative relation between the overshoot in the WT and the mutant holds true. Figures 6 and 7 are two examples of the possible behaviour of the full model under different delays. The qualitative difference between the two figures is reflected in the parameters and in the gene transcription efficiency g. Its value (for the WT) in the simulation in Fig. 6 is around 0.9, indicating nearly full induction of the genes; the corresponding value in Fig. 7, on the other hand, never rises above 0.24, indicating poor derepression for this set of parameters (data not shown).

A delay explains the experimental data if NanR displacement is inefficient

In terms of the understanding of the qualitative properties of the *N*-acetylneuraminic acid metabolic network, this points to a scenario whereby *nanATEK* is strongly repressed by NanR even in the presence of *N*-acetylneuraminic acid. This is so for the following reason: If steady-state amounts of *N*-acetylneuraminic acid could efficiently derepress *nanATEK*, then one would expect only small differences in the transient phases of the WT and the mutant because, even in the former, *nanATEK* would be derepressed; the situation is then more like the example simulations shown in Fig. 4 or Fig. 6, rather than the ones shown in Fig. 5 or Fig. 7.

This interpretation is consistent with experimental evidence reported by Kalivoda *et al.*, who used *in vitro* gel mobility experiments to demonstrate that NanR displacement by *N*-acetylneuraminic acid is inefficient.[7] However, in the same article, the authors also reported very high *in vivo* induction levels of *nanATEK* in the presence of sialic acid. Hence, overall, the evidence was somewhat contradictory. Kalivoda *et al.* speculated (and provided some experimental evidence) that the difference between the *in vivo* and the *in vitro* results might be due to the specificity of *N*-acetylneuraminic acid uptake for a specific isomer of *N*-acetylneuraminic acid (the α-isomer).

While the isomer specificity of NanT could provide a partial resolution of this contradiction, our mathematical model indicates that inefficient *nanATEK* induction by *N*-acetylneuraminic acid could be an adaptive feature with biological reality *in vivo*: At the level of the individual cell, inefficient NanR displacement means intermittent periods of *nanATEK* activation; the resulting short pulses would gradually build up enzyme levels (and *N*-acetylneuraminic acid turnover rates) and, as such, significantly reduce the risk for GlcNAc-6P accumulations.

This *ansatz* explains why the WT can avoid the toxic effect; however, it would also imply a lower steady-state *N*-acetylneuraminic acid turnover rate for the WT, and hence suboptimal nutrient utilization (suboptimal because, as the *nanR* mutant indicates, the fully derepressed phenotype is, in

steady state, fully viable while providing a higher nutrient uptake rate). This is not compatible with available experimental evidence showing similar growth rates for *nanR* mutants (taken from the inocula that are not toxic) and the WT. A possible way to circumvent this problem is a two-step induction model, whereby the initial phase of pulsed *nanATEK* activity is followed by full induction of the operon; this would require a second mechanism to effect the full induction. Such a two-step model of *nanATEK* induction could combine avoidance of toxic transient GlcNAc-6P accumulations with high steady-state *N*-acetylneuraminic acid turnover.

We propose that methylation of the NanR-binding site at the *nanA* promoter could participate in the two-step induction of the *nanATEK* operon. There are several possible scenarios as to how methylation could work. One possibility is that the methylated operator activates *nanATEK* independently of NanR binding; another is that the affinity of NanR for the methylated operator is sufficiently lowered to enable more efficient displacement by *N*-acetylneuraminic acid. Both possibilities require that (i) NanR bound to the operator acts as a methylation-blocking factor, which we know it does, and (ii) methylation of the free operator is (relatively) inefficient. As the nucleotide sequence surrounding $GATC^{NanR}$ (CCAGATCAAT) is expected to make the GATC site a relatively poor substrate for Dam methylase,[12] this second requirement also seems likely to be fulfilled.

Since we have shown that mutation of *dam* can suppress *N*-acetylneuraminic acid toxicity, our experimental evidence suggests that methylation of $GATC^{NanR}$ *per se*, rather than an effect of $GATC^{NanR}$ methylation on NanR binding, is likely to participate in the control of the *nanA* operon. However, further work is needed to determine if and how methylation of $GATC^{NanR}$ affects the expression of the *nanATEK* operon directly and to rule out the possibility that methylation does affect the affinity of NanR for its operator in the presence of *N*-acetylneuraminic acid.

Theoretically, the two-step model could work as follows: Assuming that the concentrations of *N*-acetylneuraminic acid and NanR are constant, and that the association and displacement rates for NanR are λ and γ, respectively, then the probability of *nanATEK* being repressed (at time T^r following NanR binding) or induced (at time T^i following NanR displacement) will be distributed exponentially:

$$\Pr(T^r = t) \propto \exp(-\lambda t), \quad \Pr(T^i = t) \propto \exp(-\gamma t) \quad (17)$$

Formally, the system can be modelled as a two-state continuous-time Markov chain. Then the probability of finding the system in either of its state at a given time t_k is determined by the quotient of the transition rates, that is,

$$\frac{\text{time spent in repressed state}}{\text{time spent in induced state}} = \frac{\gamma}{\lambda} \quad (18)$$

At the level of the individual cell, inefficient displacement of NanR by *N*-acetylneuraminic acid means precisely that this quotient γ/λ is very small (i.e., that *nanATEK* is repressed most of the time). This again means that there will only be short pulses of *nanATEK* expression and hence low initial rates of *N*-acetylneuraminic acid turnover, preventing GlcNAc-6P toxicity.

These short pulses of gene activity could not explain the experimentally observed full *nanATEK* induction as reported by Kalivoda *et al.* Yet, methylation could come in as a plausible second-step mechanism to effect full operon induction: Assuming a constant *N*-acetylneuraminic acid concentration, then the time to methylation T^m will again be exponentially distributed, but with the methylation rate of the unprotected GATC site modified by the probability of NanR not being bound to the operator:

$$\Pr(T^m = t) \propto \exp\left(-\frac{\gamma}{\lambda}\delta t\right) \quad (19)$$

This suggests the plausibility of a two-step model of *nanATEK* induction. During the first phase, the operon is expressed intermittently in order to slowly increase *N*-acetylneuraminic acid turnover and to avoid toxic GlcNAc-6P levels.

Conclusion

The overall picture emerging from this is as follows: Exposure of the *nanR* mutant to *N*-acetylneuraminic acid leads to a transient accumulation of GlcNAc-6P in the cell, with a toxic effect. The existence of GlcNAc-6P toxicity in *E. coli* is well documented in the literature (and corroborative evidence is reported in this contribution), although we do not currently have a mechanistic understanding of this effect. Delays in cell functions such as gene expression are a result of the GlcNAc-6P toxic effect. These delays lead to even higher transient accumulations of GlcNAc-6P, triggering a positive feedback of toxicity. Eventually, however, the GlcNAc-6P concentration will fall back to the (nontoxic) steady-state concentration. At this point, the toxic effect disappears, and cell function returns to normal. The double *nanR–nagC* mutant does not show any toxic effect because even in the absence of external *N*-acetylneuraminic acid, *nan* is fully expressed, and hence there exists no delay in gene expression and GlcNAc-6P levels are approached from below.

The WT would be susceptible to the same toxicity effect as the *nanR* mutant, unless *N*-acetylneuraminic acid turnover in the cell is initially increased significantly more slowly in the WT than in the *nanR* mutant. This could be achieved if, in *E. coli*, *nanR* displacement by *N*-acetylneuraminic acid was inefficient, only allowing intermittent activity of *nanATEK*. Such a model is consistent with measurements of the *in vitro* displacement efficiency of *N*-acetylneuraminic acid as reported by Kalivoda

et al.; however, it does not account for empirical evidence for full *nanATEK* induction *in vivo* (as suggested by the experiments reported in this contribution and by Kalivoda *et al.*).[7] In order to account for this, we predict a second mechanism that can lead to full induction of the operon after a transient period. It is likely that this second mechanism involves methylation.

Materials and Methods

Bacterial strains, plasmids, media, and growth conditions

Bacterial strains, which were all derivatives of the *E. coli* K-12 strain BGEC905, have been described in detail previously.[18]

Minimal Mops medium was prepared as described by Neidhardt *et al.* and supplemented with 10 mM thiamine, 1.32 mM phosphate, and glycerol or glucose, and/or *N*-acetylneuraminic acid was added to a final concentration of 1.11 mM.[19] All reagents were obtained from Sigma, except for *N*-acetylneuraminic acid, which was purchased from Merck Biosciences.

Cells were grown aerobically at 37 °C in minimal Mops medium, with the carbon source as indicated and subcultured to a starting OD_{600} of 0.01. Culture densities were then monitored hourly spectrophotometrically at 600 nm.

Computational simulations

The quantitative details of the system modelled by Eqs. (1)–(9) strongly depend on the particular choice of the unknown parameters. Determining these parameters either experimentally or through literature search is resource demanding, and the results are likely to be subject to large uncertainties. Hence, instead of guessing the "right" parameters of the system, the properties of the model were examined for a wide range of possible parameters.

Throughout the text, we refer to "stable" systems or models; by this, we mean a set of parameters such that, for all variables of the system, there exists at least one stable steady state. In particular, a stable system will not show unbounded growth of the concentrations of one or more molecular species.

We estimate the proportion of parameters that lead to stable models by creating a large number of random models [i.e., instantiations of the above (basic) model with random parameter values]. We check each of these models for stability and are thus able to estimate the proportion of stable models in the space of all models. For practical reasons, we limit the value of parameters to values between 0 and 1 (drawn from a uniform distribution); restricting the range of possible parameters to this interval does not limit the generality of our conclusions because we are not interested in the absolute value of the parameters, but in their relative magnitudes. All searches of the parameter space reported in this contribution were unrestricted (i.e., also included those regions of parameter space that are known to be unstable). The simulated WT was always assumed to have an arbitrary but fixed value of $nR = 0.7$.

The simulations of the transient behaviour were performed using the standard numerical integrator of the Maple9 software package. The value of s_1 was kept constant at a high (saturation level) of 4000 (arbitrary units); independent of the specific parameter values, this amount saturates the uptake mechanism in the model.

Table 4. The parameters used to simulate the extended model in Fig. 4

K_{s_1}	0.342733
V_{s_1}	0.310270
V_{e_1}	0.606901
K_{s_2}	0.452776
V_{e_2}	0.599438
k_1	0.249651
k_2	0.528698
k_3	0.474912
l_1	0.703337
l_2	0.217218
l_3	0.712827
K_c	0.395445
c_{e_2}	0.541125
c_{e_1}	0.686598
V_c	0.487362
V_{s_2}	0.372910
V_{s_0}	0.564737
K_{s_0}	0.713628

Table 5. The parameters used to simulate the extended model in Fig. 5

K_{s_1}	0.059473
V_{s_1}	0.277749
V_{e_1}	0.186220
K_{s_2}	0.159184
V_{e_2}	0.455408
k_1	0.706329
k_2	0.354706
k_3	0.134793
l_1	0.974713
l_2	0.175839
l_3	0.948983
K_c	0.067786
c_{e_2}	0.097309
c_{e_1}	0.716721
V_c	0.040482
V_{s_2}	0.863023
V_{s_0}	0.826344
K_{s_0}	0.286851

Table 6. The parameters used to simulate the full model in Fig. 6

K_{s_1}	0.848758
V_{s_1}	0.886621
V_{e_1}	0.001469
K_{s_2}	0.631901
V_{e_2}	0.665286
k_1	0.430014
k_2	0.789845
k_3	0.470588
l_1	0.799339
l_2	0.555222
l_3	0.748967
K_c	0.838957
c_{e_2}	0.137088
c_{e_1}	0.516116
V_c	0.523218
V_{s_2}	0.894033
V_{s_0}	0.517968
K_{s_0}	0.254791
c_ρ	0.075890

Table 7. The parameters used to simulate the full model in Fig. 7

K_{s_1}	0.391264
V_{s_1}	0.004042
V_{e_1}	0.137534
K_{s_2}	0.866446
V_{e_2}	0.328774
k_1	0.937549
k_2	0.195214
k_3	0.290259
l_1	0.710602
l_2	0.412784
l_3	0.179312
K_c	0.385129
c_{e_2}	0.026382
c_{e_1}	0.489789
V_c	0.721505
V_{s_2}	0.700199
V_{s_0}	0.364209
K_{s_0}	0.999872
c_ρ	0.175391

The single *nanR* mutant was simulated by setting the value of nR to 0. The *nagC* mutant was simulated by setting the value of g_2 to 1. Furthermore, in the simulations of the transient behaviour of the *nagC* mutant, the initial conditions of ϱ_{e_2} were determined as follows:

- Set the value of s_1 (external *N*-acetylneuraminic acid) to 0.
- Determine the steady-state concentrations e_2^{ss} and ϱe_2^{ss} of e_2 and ϱ_{e_2}, respectively, through simulation.
- Simulate the system again using the standard value of $s_1 = 4000$, with initial conditions of e_2 and ϱ_{e_2} set to e_2^{ss} and ϱe_2^{ss}, respectively.

Acknowledgements

I.C.B. thanks Jackie Plumbridge for discussions on *N*-acetylneuraminic acid toxicity. I.C.B. and J.R. were supported by grant 076360/Z/05/Z from the Wellcome Trust.

Appendix A. The Base Model Has, at Most, One Solution

Solving Eq. (5) gives the following expression for e_2:

$$e_2 = \frac{1}{2c_{e_2}l_1}\left(-T_1 \pm \sqrt{T_1^2 + T_2}\right) \tag{A1}$$

where $T_1 = c_{e_2}l_2 + c_{e_2}s_2l_3$ and $T_2 = 4c_{e_2}l_1V_{e_2}l_2 + 4c_{e_2}l_1V_{e_2}s_2l_3$. It is immediately clear that only the "+" solution gives physically meaningful (i.e., positive real) steady-state values for e_2. In order for the "+" solution to be positive, the expression under the square root needs to be greater than T^2. This is trivially always the case. Hence, e_2 has exactly the same number of steady-state solution as s_2.

Using computational algebra systems, it is feasible to generate explicit solutions of s_2 in terms of parameters of the system. These solutions, however, are extremely complicated and, therefore, not insightful. In the general case, s_2 will have several solutions. The relevant question in the current context is how many physically realistic (i.e., positive real) solutions s_2 has. Addressing this question does not require a full solution of s_2. From Eq. (13), we can see that s_2 only has a steady-state solution if $e_2 > e_1\alpha V_{s_2}/V_c$; here, e_1 and α can be substituted by combinations of parameters only. This means that, if the system has at least one steady state, then e_2 must be greater than some positive constant C_0 (without worrying, for the moment, about its exact value):

$$e_2 - C_0 > 0 \tag{A2}$$

Given the known expression for the steady state of e_2 from Eq. (A1) and given that we require e_2 to be positive real, we obtain:

$$-T_1 + (T_1^2 + T_2)^{1/2} > C_1 \tag{A3}$$

Again, here, $C_1 = 2c_{e_2}l_1C_0$ summarises a combination of some constant parameters. This equation means that there exists a positive constant K such that:

$$T_2^2 - 2T_1C_1 - C_1^2 - K = 0 \rightarrow s_2 = -\frac{(4c_{e_2}l_1V_{e_2}l_2 - 2c_{e_2}l_2C - 2c_{e_2}l_2K - C^2 - 2CK - K^2)}{2c_{e_2}l_3(2l_1V_{e_2} - C - K)} \tag{A4}$$

This tells us that, depending on the parameters, s_2 has either no or a unique steady-state solution; e_2 has always the same number of steady-state solutions as s_2.

The conclusion that there exists, at most, one steady state might have to be modified if one assumed additional nonlinearities in the model. These could, for example, arise from cooperativity between derepressors. We have investigated this question numerically (data not shown) and found that, over a wide range of possible cooperativity assumptions, the model still has, at most, one steady-state solution. Furthermore, whenever we found more than one steady-state solution, then there was still only one attractor solution. While our numerical experiments do certainly not amount to a mathematical proof, there is a general argument to support the conclusion: Multistability in biochemical networks is mostly associated with activators rather than with repressors.[20] Given that the interactions in this system are mostly repressive, the existence of multiple stable steady states would be unexpected. We can therefore exclude the possibility of multiple stable steady states.

We also solved a number of random instantiations of the extend model (see Materials and Methods). As theoretically predicted, we found not a single set of parameters for which there were multiple steady-state solutions. Of a sample of size of 81,000, 32.5%

leads to stable behaviour in the WT with $nR = 0.7$. Based on a sample of 33,000, an estimated 29.5% shows stable behaviour for both the WT and the NanR mutant. Finally, we found not a single instance where the WT and the double mutant were stable but the *nanR* mutant was unstable. Note that these experiments were performed over the entire parameter space, ignoring the restriction to the identified feasible values reported above.

The density of steady-state solutions for the full model crucially depends on the mRNA breakdown rate. For high mRNA breakdown rates, steady-state solutions become very sparse, particularly for longer delays. This is so because mRNA will increasingly be broken down before it could be translated; this, in turn, could lead to metabolic bottlenecks, where the efflux rate falls below the influx rate, leading to the accumulation of metabolites. Our numerical simulations have shown that, similarly to the extended model, there exists, at most, one positive real solution for the full model.

Appendix B. Derivation of Transcription Efficiencies

We assume that NanR is displaced by GlcNAc-6P in one step; that is, using the variable names from the model, we have the following reaction scheme for displacement:

$$g + nR \underset{k_2}{\overset{k_1}{\rightleftharpoons}} (1-g) \tag{B1}$$

$$(1-g) + x_1 \xrightarrow{k_3} g + x_1 + nR \tag{B2}$$

Here, g is the probability with which the relevant gene is turned on; this quantity is described by the following differential equation:

$$\dot{g} = -gnRk_2 + (1-g)k_2 + (1-g)x_1k_3 \tag{B3}$$

By setting $\dot{g} = 0$, one obtains an equation that can be solved for g:

$$g = \frac{k_2 + x_1k_3}{nRk_1 + k_2 + x_1k_3} \tag{B4}$$

References

1. Severi, E., Hood, D. & Thomas, G. (2007). Sialic acid utilization by bacterial pathogens. *Microbiology*, **153**, 2817–2822; http://dx.doi.org//009480–0.
2. Condemine, G., Berrier, C., Plumbridge, J. & Ghazi, A. (2005). Function and expression of an *N*-acetylneuraminic acid-inducible outer membrane channel in *Escherichia coli*. *J. Bacteriol.* **187**, 1959–1965.
3. Alvarez-Aorve, L., Calcagno, M. & Plumbridge, J. (2005). Why does *Escherichia coli* grow more slowly on glucosamine than on *N*-acetylglucosamine? Effects of enzyme levels and allosteric activation of GlcN6P deaminase (NagB) on growth rates. *J. Bacteriol.* **187**, 2974–2982; http://dx.doi.org/10.1128/JB.187.9.2974–2982.2005.
4. Peri, K. G., Goldie, H. & Waygood, E. B. (1990). Cloning and characterization of the *N*-acetylglucosamine operon of *Escherichia coli*. *Biochem. Cell Biol.* **68**, 123–137.
5. Plumbridge, J. (1989). Sequence of the *nagBACD* operon in *Escherichia coli* K12 and pattern of transcription within the *nag* regulon. *Mol. Microbiol.* **3**, 505–515.
6. Vimr, E. & Troy, F. (1985). Identification of an inducible catabolic system for sialic acids (*nan*) in *Escherichia coli*. *J. Bacteriol.* **164**, 845–853.
7. Kalivoda, K., Steenbergen, S., Vimr, E. & Plumbridge, J. (2003). Regulation of sialic acid catabolism by the DNA binding protein NanR in *Escherichia coli*. *J. Bacteriol.* **185**, 4806–4815.
8. Plumbridge, J. & Vimr, E. (1999). Convergent pathways for utilization of the amino sugars *N*-acetylglucosamine, *N*-acetylmannosamine, and *N*-acetylneuraminic acid by *Escherichia coli*. *J. Bacteriol.* **181**, 47–54.
9. El-Labany, S., Sohanpal, B., Lahooti, M., Akerman, R. & Blomfield, I. C. (2003). Distant *cis*-active sequences and sialic acid control the expression of *fimB* in *Escherichia coli* K-12. *Mol. Microbiol.* **49**, 1109–1118.
10. Sohanpal, B., El-Labany, S., Plumbridge, J. & Blomfield, I. (2004). Integrated regulatory responses of fimb to *N*-acetylneuraminic (sialic) acid and GlcNAc in *Escherichia coli* K-12. *Proc. Natl Acad. Sci. USA*, **101**, 16322–16327.
11. Oshima, T., Wada, C., Kawagoe, Y., Ara, T., Maeda, M., Masuda, Y. *et al.* (2002). Genome-wide analysis of deoxyadenosine methyltransferase-mediated control of gene expression in *Escherichia coli*. *Mol. Microbiol.* **45**, 673–695.
12. Peterson, S. & Reich, N. (2006). GATC flanking sequences regulate dam activity: evidence for how dam specificity may influence pap expression. *J. Mol. Biol.* **355**, 459–472.
13. Uehara, T. & Park, J. T. (2004). The *N*-acetyl-D-glucosamine kinase of *Escherichia coli* and its role in murein recycling. *J. Bacteriol.* **186**, 7273–7279; http://dx.doi.org/10.1128/JB.186.21.7273–7279.2004.
14. Vimr, E. R. & Troy, F. A. (1985). Identification of an inducible catabolic system for sialic acids (*nan*) in *Escherichia coli*. *J. Bacteriol.* **164**, 845–853.
15. Oshima, T., Wada, C., Kawagoe, Y., Ara, T., Maeda, M., Masuda, Y. *et al.* (2002). Genome-wide analysis of deoxyadenosine methyltransferase-mediated control of gene expression in *Escherichia coli*. *Mol. Microbiol.* **45**, 673–695.
16. Narang, A. (2006). Comparative analysis of some models of gene regulation in mixed-substrate microbial growth. *J. Theor. Biol.* **242**, 489–501.
17. Narang, A. & Pilyugin, S. (2007). Bacterial gene regulation in diauxic and nondiauxic growth. *J. Theor. Biol.* **244**, 326–348; http://dx.doi.org/10.1016/j.jtbi.2006.08.007.
18. Sohanpal, B., Friar, S., Roobol, J., Plumbridge, J. & Blomfield, I. (2007). Multiple co-regulatory elements and ihf are necessary for the control of *fimB* expression in response to sialic acid and *N*-acetylglucosamine in *Escherichia coli* K-12.*Mol. Microbiol.* **63**, 1223–1236; http://dx.doi.org/10.1111/j.1365–2958. 2006.05583.x.
19. Neidhardt, F., Bloch, P. & Smith, D. (1974). Culture medium for enterobacteria. *J. Bacteriol.* **119**, 736–747.
20. Alon, U. (2006). *An Introduction to Systems Biology: Design Principles of Biological Circuits.* Chapman and Hall.